Conversion of the Conduction Type of a Catalytic-Chemical-Vapor-Deposited p-type a-Si by PH_3 Plasma Ion Implantation

Huynh-Thi-Cam Tu[1], Koichi Koyama[1,*], Noboru Yamaguchi[2], Hideo Suzuki[2], Keisuke Ohdaira[1], Hideki Matsumura[1]

[1]Japan Advanced Institute of Science and Technology, Nomi, Ishikawa, 923-1292, Japan.

[2]ULVAC Inc., Susono, Shizuoka 410-1231, Japan

[*]Present address: ULVAC, Inc., Chigasaki, Kanagawa 253-8543, Japan

Corresponding author: Huynh Thi Cam Tu, tu-huynh@jaist.ac.jp, +84-761-51-1187, Japan Advanced Institute of Science and Technology, Nomi, Ishikawa 923-1292, Japan.

Abstract

In this work, we propose counter-doping into a p-type amorphous silicon (a-Si) film prepared by catalytic chemical vapor chemical deposition (Cat-CVD) by PH_3 plasma ion implantation (PII). This method is expected to simplify the formation of p-n patterns in the back-side electrodes of interdigitated back contacted amorphous silicon (a-Si)/crystalline silicon (c-Si) heterojunction (IBC-SHJ) solar cells. In particular, we investigate the effect that hydrogen atoms implanted together with phosphorous dopants during PH_3 PII have on the surface passivation properties of counter-doped p-a-Si on c-Si. Conversion in the conduction type of p-a-Si after PH_3 PII is confirmed by the operation of SHJ solar cells.

Keywords:

Catalytic vapor deposition, Plasma Ion Implantation, Interdigitated back-contact silicon heterojunction solar cell, back-side contacts; counter doping; Amorphous silicon

1. Introduction

Photovoltaic (PV) energy has attracted immense interest in recent years as an alternative source of electrical energy to mitigate climate change. In 2017, PV electricity generation was 443 TWh, corresponding to approximately 1.7% of global electricity generation [1]. Currently, most commercial PV cells are based on crystalline silicon (c-Si) wafers and account for aproximately 95% of total production [1]. By improving manufacturing technology, the efficiency of c-Si solar cells has been increasing steadily. In particular, the combination of the amorphous silicon (a-Si)/c-Si heterojunction (SHJ) with the interdigitated back-contact (IBC), known as the IBC-SHJ, has resulted in conversion efficiencies as high as 26.7% [2, 3]. However, the fabrication of IBC-SHJ cells is considered complex, particularly for the back-side contact formation process [4]. To further reduce manufacturing costs and lower the price of the solar cell, a decrease in the number of cell fabrication process steps is required. For this purpose, we have developed a method to make back-side contact fabrication easy and simple. In this method, we use plasma ion implantation (PII) with a precursor phosphine (PH_3) gas to implant phosphorous (P) ions into p-type a-Si prepared by catalytic chemical vapor chemical deposition (Cat-CVD) [5] and convert its conduction type to n-type. PII and a hard mask are used to convert some patterned areas from p-a-Si to n-a-Si, as illustrated in Fig. 1, which appears to be a very promising method to reduce the manufacturing cost of IBC-SHJ cells. In addition, the a-Si films were prepared by Cat-CVD, which provides a good a-Si/c-Si interface due to its free plasma induced damage properties [6]. Therefore, a high quality surface passivation of the c-Si using Cat-CVD a-Si is expected to be obtained.

We have already reported some preliminary results concerning the application of PH_3 PII into Cat-CVD p-type a-Si films for conversion to n-type conduction [7]. We have confirmed that after ion implantation and due to implantation damages, the passivation quality of a-Si on c-Si is significantly degraded and by applying an anneal at a temperature of approximately 250 °C, the surface passivation quality of a-Si can be restored [8]. Indeed, annealing appears to be a key process for removing implantation damage. However, there still remains the question of why the implantation damage can be removed by an annealing process at a temperature as low as 250 °C, whereas in conventional ion implantation (CII)

into c-Si, the typical annealing temperatures required are 800–1,000 °C are usually required. In this paper, we reveal the effect of annealing on the surface passivation quality of n-a-Si formed by PH_3 PII on c-Si to answer this question.

2. Experimental Procedure

2.1 Preparation of samples for evaluating surface passivation quality

Fig. 2(a) shows the schematic structure of the samples for evaluating the surface passivation quality of a-Si on c-Si after PII. The n-type mirror-polished 300-μm-thick (100) float-zone c-Si wafers with a resistivity of 1–5 Ωcm were immerged in a 5wt% diluted hydrofluoric acid (HF) solution for 30 s to remove native oxide layers on their surfaces and then in a 4wt% diluted peroxide (H_2O_2) solution for 30 s to form ultrathin oxide layers on their surfaces to avoid any epitaxial growth during a-Si film deposition [9, 10]. Then, on the front side of the c-Si wafers, intrinsic a-Si (i-a-Si)/silicon nitride (SiN_x) stacked passivation layers were formed by Cat-CVD to obtain a surface recombination velocity as low as 0.18 cm/s [11, 12] and to simulate the same architecture that is present on the front side of the IBC-SHJ cell. On the rear side of the c-Si, i-a-Si/p-a-Si stacked layers with individual layer thicknesses of ~10 nm were deposited by Cat-CVD. Furthermore, samples with a structure of 20-nm-thick i-a-Si/n-type c-Si/i-a-Si/SiN_x were prepared. The deposition conditions of the a-Si and SiN_x films by Cat-CVD are summarized in Table I. The P and H ions were then implanted into i-a-Si or p-a-Si films by PII or CII. Finally, the samples were annealed in an air atmosphere. The surface passivation quality of the a-Si films on c-Si before and after ion implantation was evaluated by measuring the effective carrier lifetime using the microwave photoconductive decay method (μ-PCD; KOBELCO LTA-1510EP) with a laser light wavelength of 904 nm and an area photon density of 5×10^{13} cm^{-2}.

2.2 Preparation of the SHJ solar cell

To confirm the conversion of the conduction type of p-a-Si after PH_3 PII, we prepared SHJ-like solar cells, as shown in Fig. 2 (b). The n-type mirror-polished 300-μm-thick (100) float-zone c-Si wafers with a resistivity of 1–5 Ωcm were used. After dipping the c-Si in the HF and H_2O_2 solutions described above,

both sides of the c-Si were coated with Cat-CVD i-a-Si/p-a-Si staked layers with individual layer thicknesses of ~10 nm. The PH_3 PII was performed to implant P ions into one of the two i-a-Si/p-a-Si stacked layers. Then, the samples were annealed in air at 240 °C for 100 min prior to forming indium tin oxide (ITO) and Ag finger electrodes by sputtering and thermal evaporation, respectively. Before measuring the current density–voltage (*J*–*V*) characteristics, post-annealing in air at 200 °C for 30 min was carried out.

2.3 Ion implantation conditions

The PII was performed in an ULVAC PVI-3000 PII system equipped with no mass-separator. The configuration of the PII system is described in [13]. PH_3 was used as the precursor gas. Since there is no mass-separator, all the P^+, H^+, and PH_x^+ ions produced by the plasma decomposition of the PH_3 gas are expected to be implanted into the a-Si. The ion implantation energy and ion dose density were maintained at 5 keV and 1×10^{16} cm^{-2}, respectively. However, to maintain the substrates at approximately room temperature, the substrates were implanted twice at an ion dose of 5×10^{15} cm^{-2}. The duration of each implantation was ~1.7 s.

The CII was carried out in an ULVAC SOPHI-260 system equipped with a mass-separator. PH_3 was again used as precursor gas. The samples were maintained at room temperature during implantation with an ion energy and an ion dose of 5 keV, and 1×10^{16} cm^{-2}, respectively. Since the mass-separator type ion implantation system has a low beam current, a time of ~8 h was required to implant the P or H ions at an ion dose of 1×10^{16} cm^{-2}.

3. Results and Discussion

Fig. 3 shows the effective carrier lifetime before and after the PH_3 PII of the two samples: (20 nm) i-a-Si/c-Si/i-a-Si/SiN_x and (10 nm) p-a-Si/(10 nm) i-a-Si/c-Si/i-a-Si/SiN_x. A significant decrease in the carrier lifetime after PII is considered to be the result of implant-induced damage [8, 14]. By applying the annealing treatment, the carrier lifetimes of these samples were dramatically increased. It is clearly seen that the carrier lifetime strongly depends on the temperature and the duration of annealing process. The

peaks of the carrier lifetime likely shift to a high temperature as the annealing time decreases. An appropriate annealing procedure should therefore be considered in order to obtain an a-Si film with high-quality surface passivation after PII.

Fig. 4 shows secondary ion-mass spectrometry (SIMS) depth profiles of the H, P and B in 10-nm-thick-p-a-Si/10-nm-thick-i-a-Si/c-Si samples before and after PH_3 PII. The SIMS profiles were obtained by measuring from the c-Si side to the a-Si side to suppress knock-on effects. For the sample after PII, H atoms with concentration of 10^{20} cm^{-3} are seen at a depth of 50 μm in the c-Si regions and P atoms with a concentration in excess of 10^{20} cm^{-3} are found at a depth of 10 nm near the a-Si surface regions and likely decrease to 10^{18} cm^{-3} at the a-Si/c-Si interface. This result indicates that for PII system, the H ions produced by plasma decomposition of the PH_3 precursor gas were implanted together with the P ions.

Fig. 5 shows the SIMS depth profiles of the H atoms in 20-nm-thick-a-Si/c-Si after PH_3 PII and successive annealing at 250 °C for 210 min in air. The concentration of the implanted H atoms in the c-Si after annealing at 250 °C was slightly decreased. We already confirmed that the concentration of the implanted P atoms was not changed by annealing [8]. The implanted H atoms likely diffused out of the c-Si to the a-Si/c-Si interface and then effused from the a-Si films during the annealing process. Returning to the lifetime results shown in Fig. 3, we see that the improvement in the carrier lifetime resulting from the annealing at 250 °C seems to be strongly related to these H atoms.

To confirm the effect of the H atoms, we carried out the ion implantation of P ions alone and P ions with the addition of H ions at an ion energy of 5 keV and at ion doses of 10^{15} and 10^{16} cm^{-2} to 20-nm-thick i-a-Si/n-type c-Si/i-a-Si/SiN_x by CII and observed their carrier lifetimes. Fig. 6(a) shows the lifetime results of these samples before and after implantation and after implantation and annealing at 250 °C for 210 min. For comparison, we added the carrier lifetime results of the sample with the same structure, but where the i-a-Si film was treated by PH_3 PII. The results clearly show that the carrier lifetimes of the samples implanted with an additional H increased after annealing. This result indicates that the implanted H atoms play a key role in healing the damage caused by the implantation process. However,

it should be noted that carrier lifetime after annealing the sample implanted with P and H ions at an ion dose of 10^{16} cm^{-2} was only 171 μs, which is three times less than the sample implanted with P and H ions at an ion dose of 10^{15} cm^{-2}. It is considered that implantation at an ion dose of 10^{16} cm^{-2} may induce severe damage that is difficult to heal using H atoms.

Fig. 6(b) shows the SIMS depth-profiles of the H atoms of the above samples, particularly the samples after implantation and annealing. In the SIMS results, we note that although the PII and CII were carried out under the same conditions, (an ion energy of 5 keV and an ion dose of 10^{16} cm^{-2}), the concentration and penetration depth of the H atoms implanted in the c-Si by PII are much lower and shorter than those implanted by CII. This result could be explained by two main reasons. First, for PII, the ion dose of 10^{16} cm^{-2} accounts for all the ions produced by the plasma decomposition of the PH_3 gas. We have confirmed that at an ion dose of 10^{16} cm^{-2} the dose of H ions is approximately 5×10^{15} cm^{-2}. In the case of CII, the ion dose of 10^{16} cm^{-2} is only for the H ions. Hence, for the same setup ion dose (i.e., 10^{16} cm^{-2}), the concentration of H atoms in the c-Si implanted by the PII system is less than that implanted by the CII system. Second, collisions inside the plasma sheath cause the energy of the H ions to be decreased (i.e., less than 5 keV). This decrease can lead to the penetration depth of the H atoms implanted by the PII system to be less than those implanted by the CII system.

Fig. 6(b) also shows that the concentration of H in the c-Si treated by CII at an ion dose of 10^{16} cm^{-2} was much more than the concentration at an ion dose of 10^{15} cm^{-2}. As greater number of H atoms are implanted in the c-Si, more damage is produced in the c-Si and the a-Si/c-Si interface. Since the longest carrier lifetime (1 ms) is obtained for the sample receiving the PH_3 PII treatment with a peak concentration of H atoms in the c-Si of less than 10^{20} cm^{-3}, it is believed that there is a trade-off correlation between the passivation effect and the damage by H atoms implanted in the c-Si.

As shown in Fig. 6(a), the carrier lifetime was dramatically decreased just after ion implantation. This phenomenon is considered to be due to the implantation-induced-damages. Dangling-bond-type-defects at a-Si/c-Si interface are assumed to be one of the damages-type caused by the implantation of

P and/or H ions. It is assumed that during the annealing process, the H atoms implanted in the c-Si diffuse out of the c-Si (see Fig. 5). This diffusion process is considered as a transfer of H from the c-Si to the a-Si/c-Si interface, which contributes to the termination of the dangling bonds on the c-Si surface [15-17]. In other words, due to the implanted H atoms, good passivation can be achieved even at annealing temperature as low as 250 °C. The PH_3 PII appears to be a promising implantation method, since the P dopants and the H atoms are implanted simultaneously.

Fig. 7 shows the H_2 desorption data from the p-a-Si/i-a-Si/c-Si before and after PH_3 PII as a function of heating temperature. The data were taken from a thermal desorption spectroscopy (TDS) measurement at a temperature rate of 30 °C/min. The H_2 desorption characteristics of a-Si/c-Si systems before and after PH_3 PII are rather similar. A broadened hydrogen desorption peak centered at ~300 °C is confirmed in both samples. Wolf and Kondo have stated that the desorption of H atoms from a-Si cause dangling-bond-type defects [18], which may lead to degradation in the surface passivation quality. The reduction in carrier lifetime (Fig. 3) by annealing at high temperatures (e.g., above 300 °C for 5 min) after PH_3 PII can be interpreted to be caused by the H desorption phenomenon.

Fig. 8 shows the photo *J*–*V* characteristics of the samples with two structures: Ag/ITO/p-a-Si/i-a-Si/n-c-Si/i-a-Si/p-a-Si/ITO/Ag (before PH_3 PII) and Ag/ITO/p-a-Si/i-a-Si/n-c-Si/i-a-Si/PH_3-implanted-p-a-Si/ITO/Ag (after PH_3 PII). The sample with p-a-Si implanted by PH_3 PII exhibits photo *J*–*V* characteristics that are typical of a solar cell. Although the cell efficiency was approximately 12.5 %, we can confirm that the conduction of p-type a-Si was converted to the n-type after PH_3 PII and a subsequent annealing at 240 °C for 100 min.

4. Conclusions

PH_3 PII was conducted to counterdope the p-type a-Si prepared by Cat-CVD to n-type a-Si. The effect of annealing on the surface passivation quality of the n-a-Si film on n-c-Si was investigated. It was found that during PII process, the H ions produced by the plasma decomposition of the PH_3 precursor gas were implanted together with the P ions. These implanted H atoms play a key role in terminating the

dangling bonds caused by the implantation process, resulting in an improvement in the surface passivation quality of the n-a-Si. To avoid degradation in the passivation quality caused by the out-diffusion of the H atoms, any annealing should be performed after PII at temperatures below 325 °C.

Acknowledgement

This work was financially supported by the New Energy and Industrial Technology Development Organization (NEDO), Japan.

References

[1] Fraunhofer Institute for Solar Energy Systems, Dr. Simon Philipps, Werner Warmuth, Photovoltaics Report. [Internet]. Updated 27 August 2018.

https://www.ise.fraunhofer.de/content/dam/ise/de/documents/publications/studies/Photovoltaics-Report.pdf

[2] K. Yoshikawa, H. Kawasaki, W. Yoshida, T. Irie, K. Konishi, K. Kanako, T. Uto, D. Adachi, M. Kanemastu, H. Uzu, and K. Yamamoto, Silicon heterojunction solar cell with interdigitated back contacts for a photoconversion efficiency over 26%, Nat. Energy 2 (2017) 17032

[3] K. Yoshikawa, W. Yoshida, T. Irie, H. Kawasaki, K. Konishi, H. Ishibashi, T. Asatani, D. Adachi, M. Kanematsu, H. Uzu, K. Yamamoto, Exceeding conversion efficiency of 26% by heterojunction interdigitated back contact solar cell with thin film Si technology, Sol. Energy Mater. Sol. Cells, 173 (2017) 37

[4] J. Nakamura, N. Asano, T. Hieda, C. Okamoto, H. Katayama, and K. Nakamura, Development of Heterojunction Back Contact Si Solar Cells, IEEE J. Photovoltaics 4 (2014) 1491

[5] H. Matsumura, Study on catalytic chemical vapor deposition method to prepare hydrogenated amorphous silicon, J. Appl. Phys. 65, (1989) 4396.

[6] H. Matsumura, K. Higashimine, K. Koyama, and K. Ohdaira, Comparison of crystalline-silicon/amorphous-silicon interface prepared by plasma enhanced chemical vapor deposition and catalytic chemical vapor deposition, J. Vac. Sci. Technol. B 33, (2015) 31201.

[7] K. Koyama, K. Ohdaira, H. Matsumura, Entrance of Low Cost Fabrication of Back-Contact Heterojunction Solar Cells by Using Plasma Ion Implantation in 2017 44 th IEEE Photovoltaic Specialist Conference, PSCV (2017) 1787-1789.

[8] K. Koyama, N. Yamaguchi, D. Hironiwa, H. Suzuki, K. Ohdaira, H. Matsumura, Simple fabrication of back contact hetero-junction solar cells by plasma ion-implantation, Jpn. J. Appl. Phys. 56 (2017) 08MB21

[9] T. Oikawa, K. Ohdaira, K. Higashimine, and H. Matsumura, Application of crystalline silicon surface oxidation to silicon heterojunction solar cells, Curr. Appl. Phys. 15 (2015) 1168

[10] K. Ohdaira, T. Oikawa, K. Higashimine, and H. Matsumura, Suppression of the epitaxial growth of Si films in Si heterojunction solar cells by the formation of ultra-thin oxide layers, Curr. Appl. Phys. 16, (2016) 1026.

[11] K. Koyama, K. Ohdaira, and H. Matsumura, Extremely low surface recombination velocities on crystalline silicon wafers realized by catalytic chemical vapor deposited SiN_x/a-Si stacked passivation layers, Appl. Phys. Lett. 97 (2010) 082108.

[12] C. T. Nguyen, K. Koyama, S. Terashima, C. Okamoto, S. Sugiyama, K. Ohdaira, and H. Matsumura, Novel chemical cleaning of textured crystalline silicon for realizing surface recombination velocity < 0.2 cm/s using passivation catalytic CVD SiNx /amorphous silicon stacked layers, Jpn. J. Appl. Phys. 56 (2017) 056502.

[13] K. Nakamura, K. Muramatsu, N. Yamaguchi, Y. Ohshita, Non Mass Separation Type Ion Implantation System for Bifacial PERT Cell Fabrication in 35th European Photovoltaic Solar Energy Conference and Exhibition, pp 375 – 378, 10.4229/35thEUPVSEC20182018-2BO.3.5

[14] T. Carrere, D. Munoz, M. Coig, C. Longeaud, and J-P Kleider, p-type a-Si:H doping using plasma immersion ion implantation for silicon heterojunction solar cell application, Sol. RRL 1 (2017) 1600007.

[15] S. De Wolf, S. Olibet and C. Ballif, Stretched-exponential a−Si:H/c−Si interface recombination decay, Appl. Phys. Lett. 93 (2008) 032101.

[16] T. F. Schulze, H. N. Beushausen, C. Leendertz, A. Dobrich, B. Rech and L. Korte, Interplay of amorphous silicon disorder and hydrogen content with interface defects in amorphous/crystalline silicon heterojunctions, Appl. Phys. Lett. 96 (2010) 252102.

[17] C. Leendertz, N. Mingirulli, T. F. Schulze, J. P. Kleider, B. Rech and L. Korte, Discerning passivation mechanisms at a-Si:H/c-Si interfaces by means of photoconductance measurements, Appl. Phys. Lett. 98 (2011) 202108.

[18] S. D. Wolf, and M. Kondo, Nature of doped a-Si:H/c-Si interface recombination, J. Appl. Phys. 105 (2009) 103707

Figure and table captions:

Figure 1: PH_3 PII with a hard mask to convert some patterns areas from p-a-Si to n-a-Si

Figure 2: Schematic structures of (a) the samples for measuring carrier lifetime and (b) SHJ solar cells.

Figure 3: (a) Carrier lifetime of samples with (20 nm) i-a-Si/c-Si/i-a-Si/SiN_x and (10 nm) p-a-Si/(10 nm) i-a-Si/c-Si/i-a-Si/SiN_x structures after PH_3 PII and subsequent annealing for 60 min. (b) Carrier lifetime of samples with a (20 nm) i-a-Si/c-Si/i-a-Si/SiN_x structure after PH_3 PII and subsequent annealing for 5, 30 and 60 min.

Figure 4: SIMS depth-profile of the H, P and B atoms in p-a-Si/i-a-Si/c-Si after PH_3 PII at an implantation energy of 5 keV and an ion dose of 10^{16} cm^{-2}.

Figure 5: SIMS depth-profile of H in 20-nm-i-a-Si/c-Si after PH_3 PII at an implantation energy of 5 keV and an ion dose of 10^{16} cm^{-2} with and without annealing at 250 °C for 210 min.

Figure 6: (a) Effective carrier lifetime of samples with a 20-nm-thick i-a-Si/c-Si/i-a-Si/SiN_x structure under mass-separated implantation of P alone and P with the addition of H at an implantation energy of 5 keV. Annealing was performed at 250 °C for 210 min. (b) SIMS depth-profile of H in the samples after implantation and annealing.

Figure 7: Intensity of H_2 (molecular weight = 2) from the TDS analysis of p-i-a/i-a-Si/c-Si after PH_3 PII

Figure 8: Photo J-V characteristics of the samples with two structures; Ag/ITO/p-a-Si/i-a-Si/n-c-Si/i-a-Si/p-a-Si/ITO/Ag (before PH_3 PII) and Ag/ITO/p-a-Si/i-a-Si/n-c-Si/i-a-Si/PH_3-implanted-p-a-Si/ITO/Ag (after PH_3 PII).

Table 1: Parameters for the Cat-CVD film deposition and thickness (*t*)

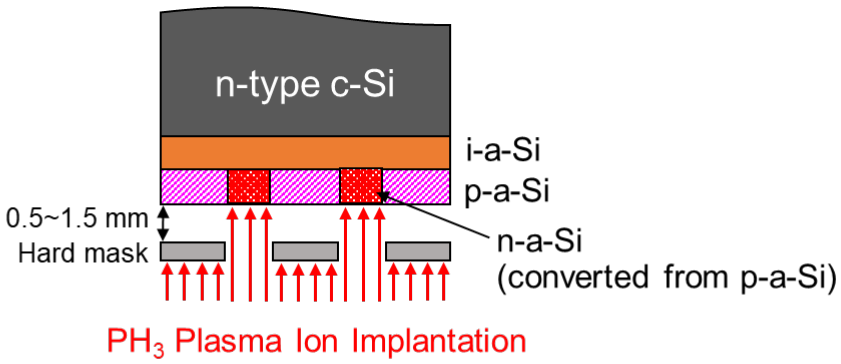
n-type c-Si
i-a-Si
p-a-Si
0.5~1.5 mm
Hard mask
n-a-Si
(converted from p-a-Si)
PH3 Plasma Ion Implantation

Figure 1

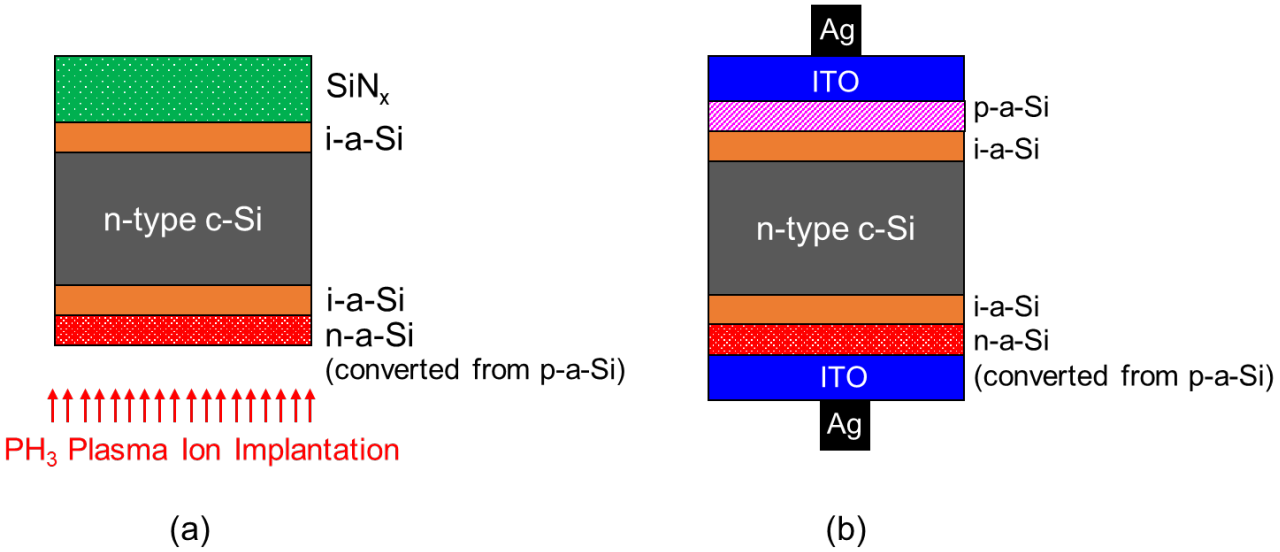
SiNx
i-a-Si
n-type c-Si
i-a-Si
n-a-Si
(converted from p-a-Si)
PH3 Plasma Ion Implantation
(a)
Ag
ITO
p-a-Si
i-a-Si
n-type c-Si
i-a-Si
n-a-Si
(converted from p-a-Si)
ITO
Ag
(b)

Figure 2

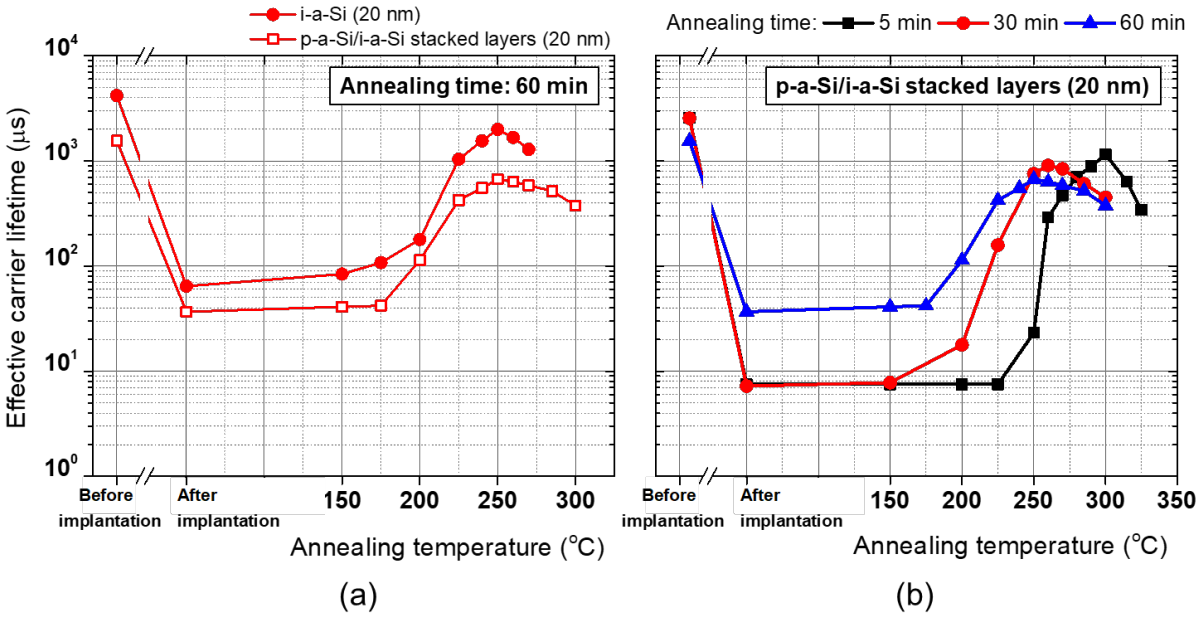
i-a-Si (20 nm)
p-a-Si/i-a-Si stacked layers (20 nm)
Annealing time: 60 min
Effective carrier lifetime (μs)
Before implantation
After implantation
Annealing temperature (°C)
(a)
Annealing time: 5 min 30 min 60 min
p-a-Si/i-a-Si stacked layers (20 nm)
Before implantation
After implantation
Annealing temperature (°C)
(b)

Figure 3

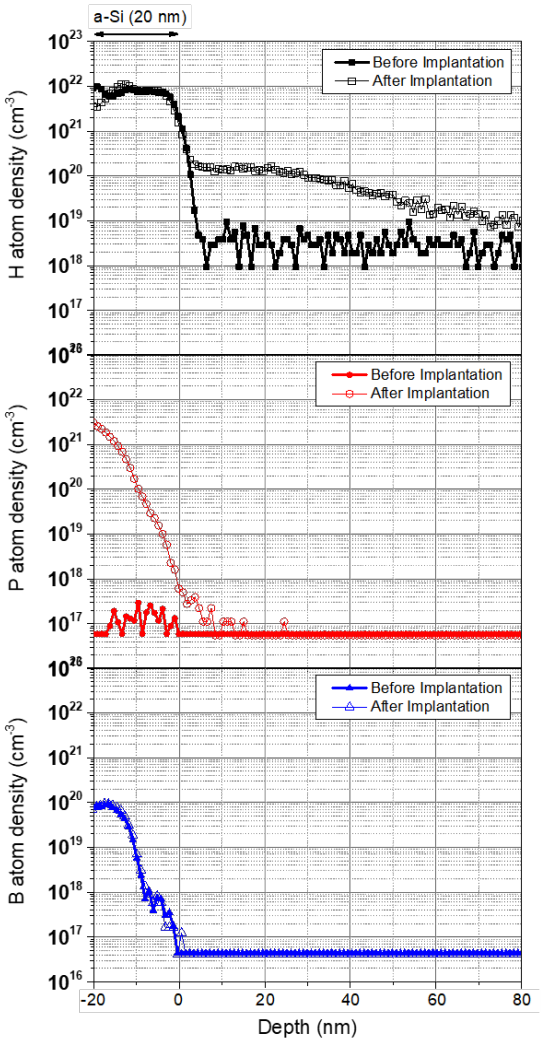
a-Si (20 nm)
H atom density (cm-3)
P atom density (cm-3)
B atom density (cm-3)
Before Implantation
After Implantation
Depth (nm)

Figure 4

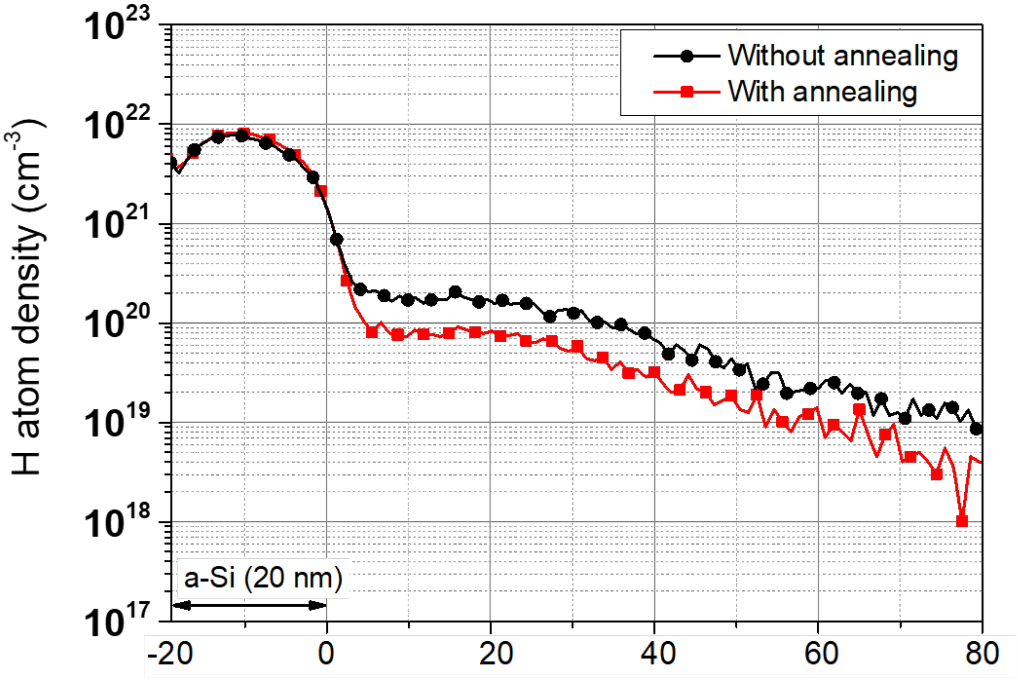
Without annealing
With annealing
H atom density (cm-3)
10^23
10^22
10^21
10^20
10^19
10^18
10^17
a-Si (20 nm)
-20
0
20
40
60
80

Figure 5

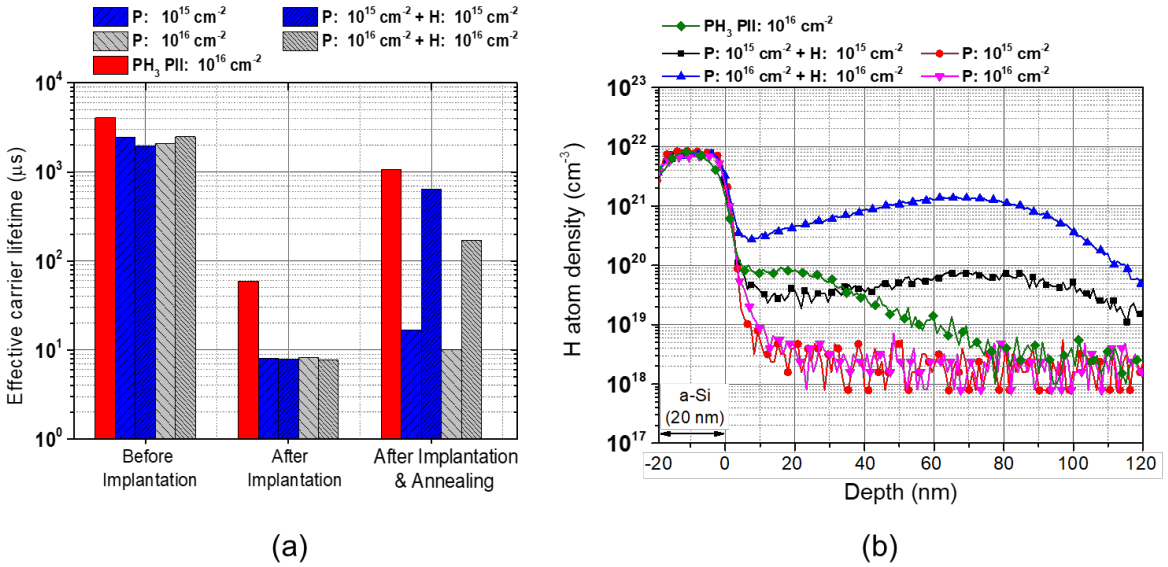
P: 10^15 cm^-2
P: 10^15 cm^-2 + H: 10^15 cm^-2
P: 10^16 cm^-2
P: 10^16 cm^-2 + H: 10^16 cm^-2
PH3 PII: 10^16 cm^-2
Effective carrier lifetime (μs)
Before Implantation
After Implantation
After Implantation & Annealing
(a)
PH3 PII: 10^16 cm^-2
P: 10^15 cm^-2 + H: 10^15 cm^-2
P: 10^15 cm^-2
P: 10^16 cm^-2 + H: 10^16 cm^-2
P: 10^16 cm^-2
H atom density (cm^-3)
a-Si (20 nm)
Depth (nm)
(b)

Figure 6

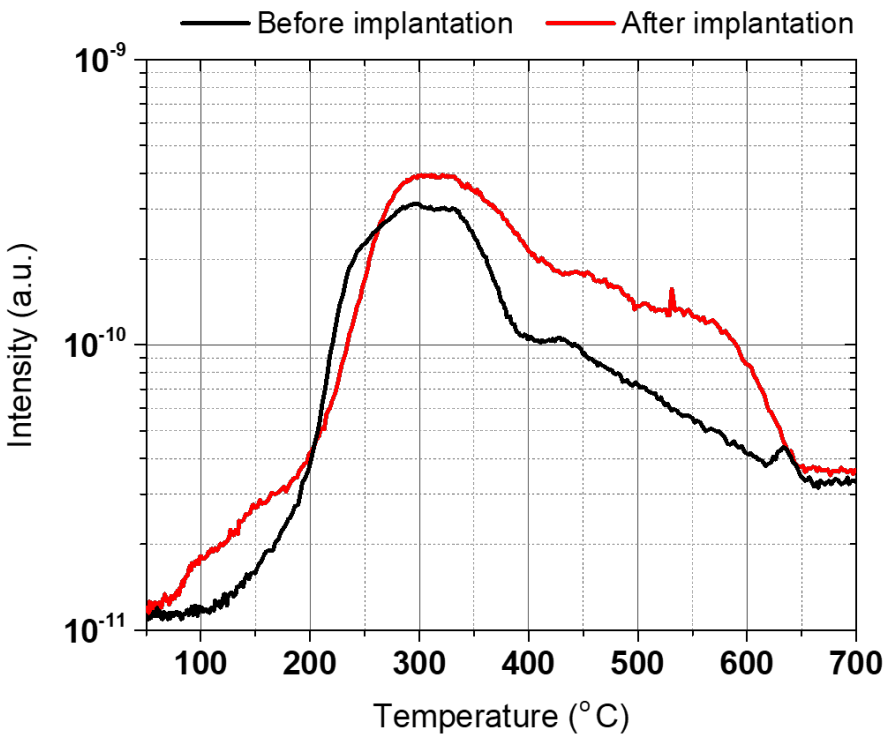
Before implantation
After implantation
Intensity (a.u.)
10-9
10-10
10-11
100
200
300
400
500
600
700
Temperature (°C)

Figure 7

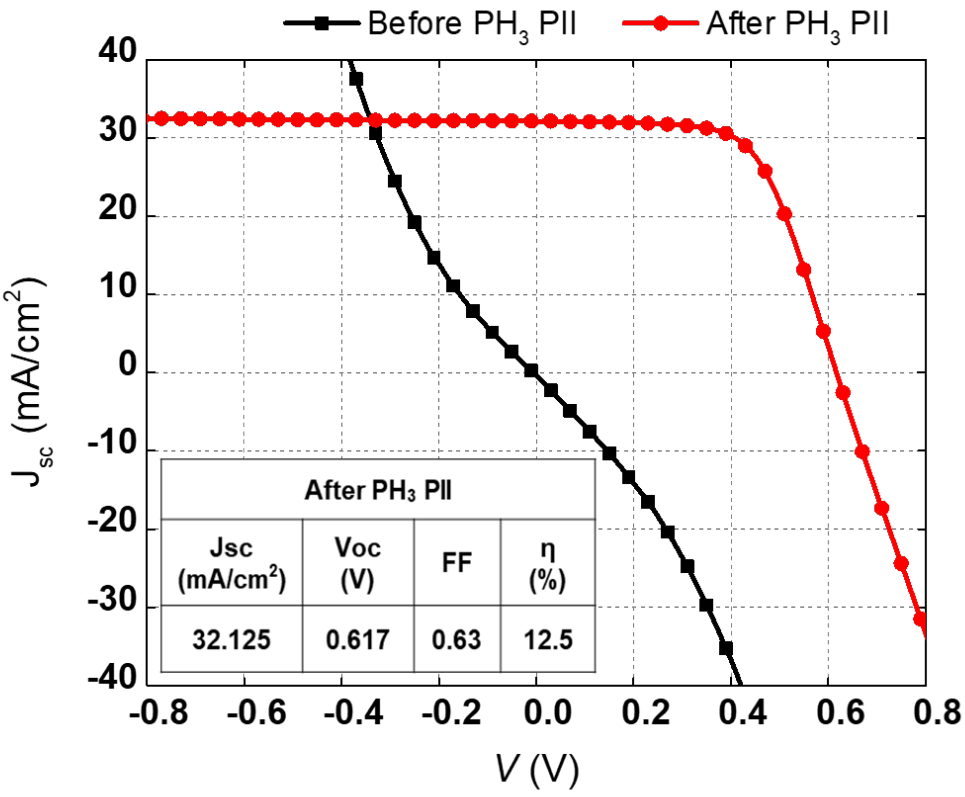
Before PH3 PII
After PH3 PII
40
30
20
10
0
-10
-20
-30
-40
-0.8
-0.6
-0.4
-0.2
0.0
0.2
0.4
0.6
0.8
Jsc (mA/cm2)
V (V)
After PH3 PII
Jsc (mA/cm2)
Voc (V)
FF
η (%)
32.125
0.617
0.63
12.5

Figure 8